Herrick Laboratories
PURDUE UNIVERSITY

2016 Purdue Conferences
Compressor Engineering
Refrigeration and Air Conditioning
High Performance Buildings

Analysis on Lubricant Film Force for Two Types of Meshing Pair Profile in Single Screw Compressor

Feilong Liu

School of Energy and Power Engineering, Xi’an Jiaotong University,

Xi’an, Shaanxi, China

Department of Flow, Heat, and Combustion Mechanics, Ghent University,

Ghent, Belgium

liufeilong@stu.xjtu.edu.cn

July 11 -14, 2016

PURDUE UNIVERSITY

Center for High Performance Buildings at Purdue

1. INTRODUCTION

Single screw compressor

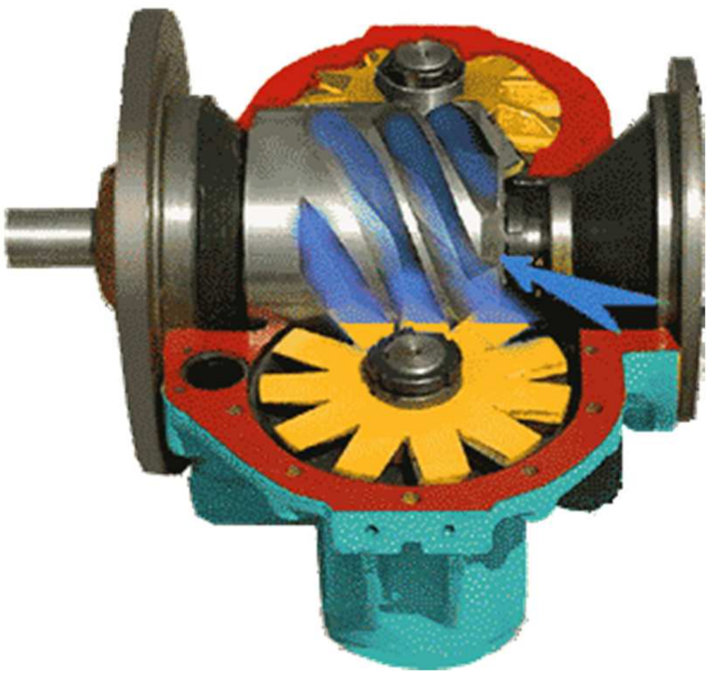

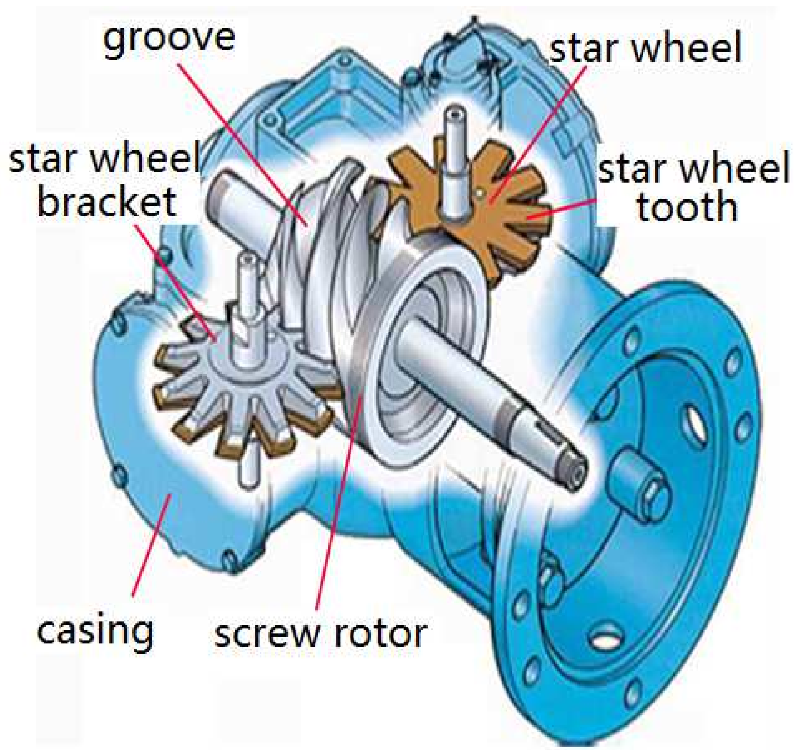

1. INTRODUCTION

- Profile of the envelope meshing pair

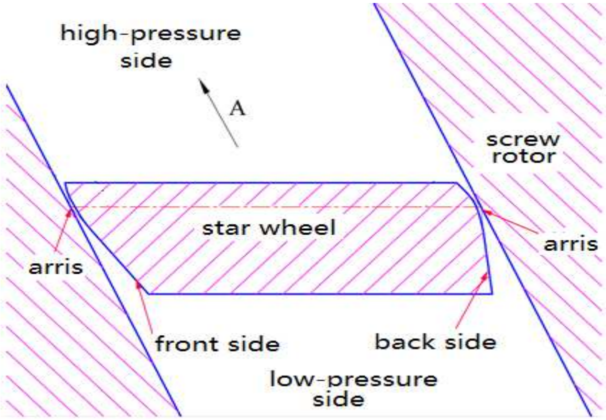

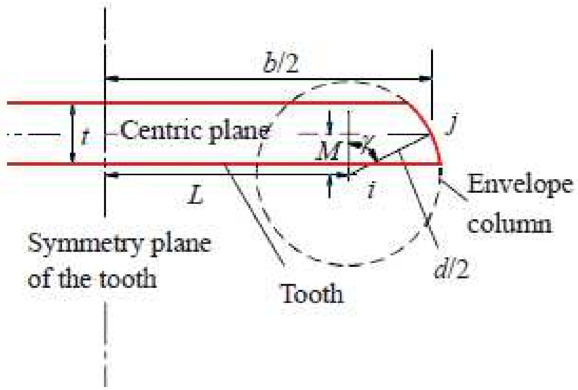

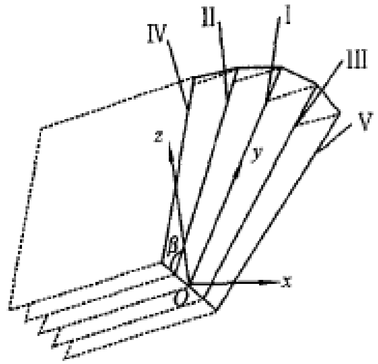

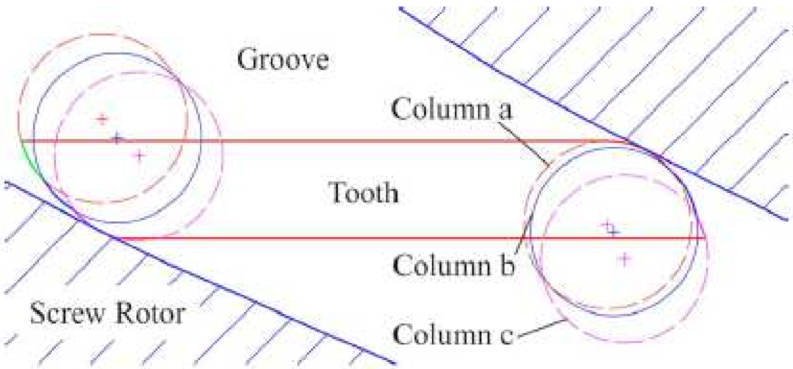

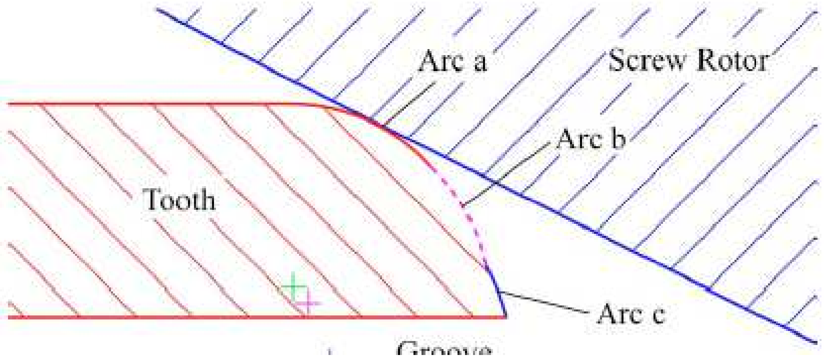

1. INTRODUCTION

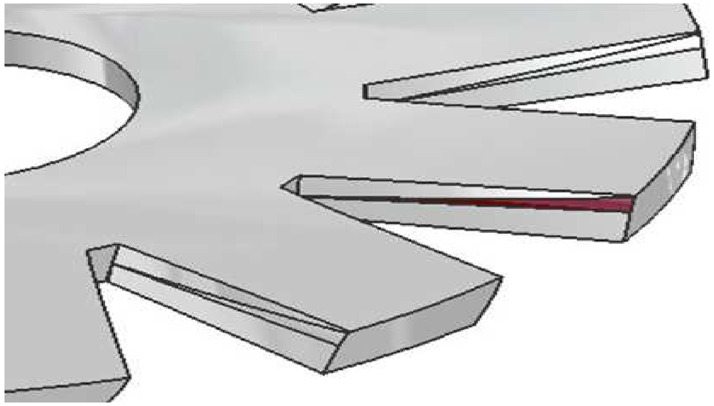

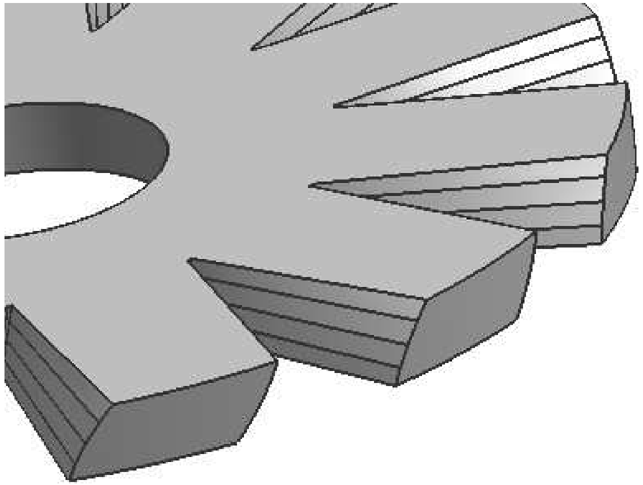

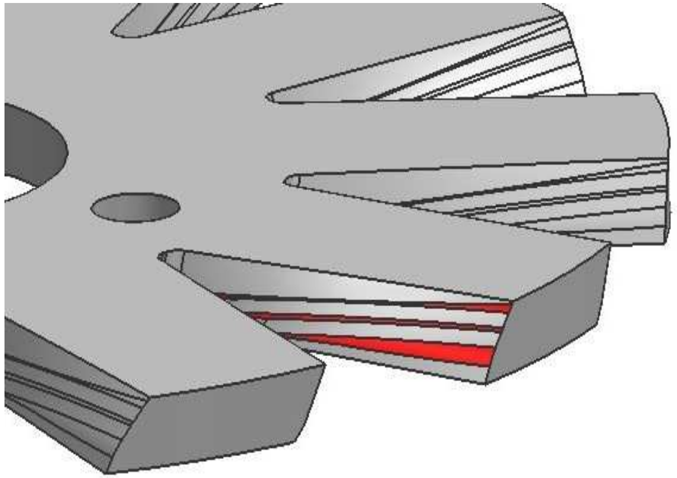

1. INTRODUCTION

- Lubrication between the meshing pair

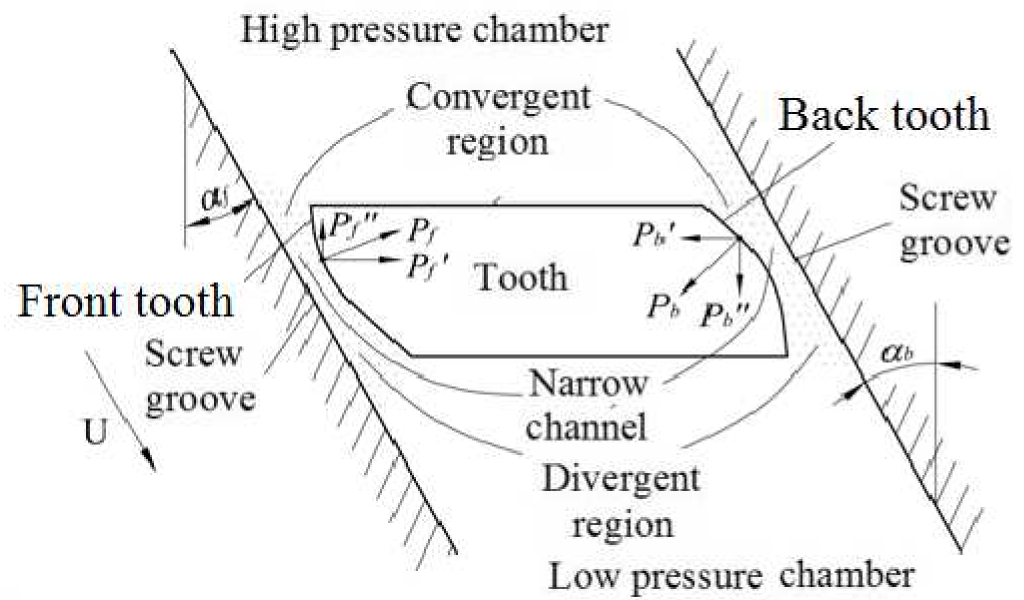

2. GEOMETRY MODEL

- **2.1 Geometric and Kinematic Relations Between The Meshing Pair**

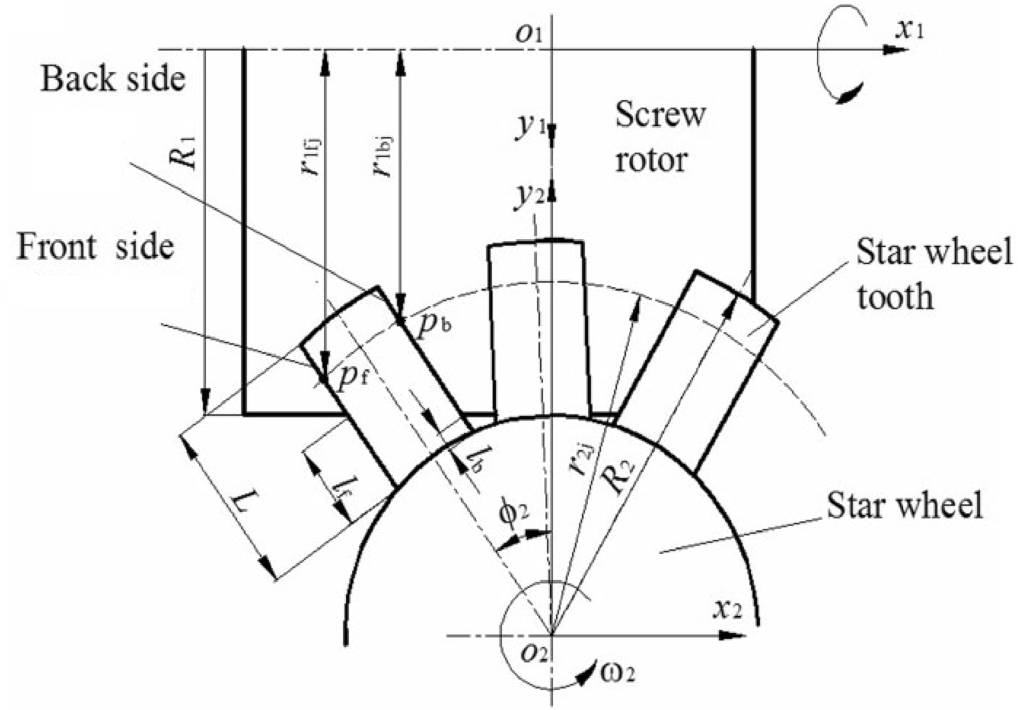

2. GEOMETRY MODEL

- the related swinging radius r_{2j} is

$$r_{2j} = \sqrt{\left(\sqrt{R_2^2 - (b/2)^2} - (L-l)\right)^2 - (b/2)^2}$$

- The swinging radius from the contact point to the rotor center, r_{1fj} and r_{1b}

$$\begin{cases} r_{1fj} = a - r_{2j}\cos(\phi_2 + \delta) \\ r_{1bj} = a - r_{2j}\cos(\phi_2 - \delta) \end{cases} \qquad \delta = \arccos(\frac{b}{2R_2})$$

- The unengaged length on both sides of the tooth l_f and l_b

$$\begin{cases} l_f = L - \dfrac{R_2 \cdot \cos(\delta + \phi_2) - a + R_1}{\cos\phi_2} \\ l_b = L - \dfrac{R_2 \cdot \cos(\delta - \phi_2) - a + R_1}{\cos\phi_2} \end{cases}$$

2. GEOMETRY MODEL

- **2.2 Double-column Meshing Pair**

  - The groove inclined angles

$$\begin{cases} \tan\alpha_{f1} = \dfrac{\omega_2 r_{2j}}{\omega_1 r_{1fj}} \\ \tan\alpha_{b1} = \dfrac{\omega_2 r_{2j}}{\omega_1 r_{1bj}} \end{cases}$$

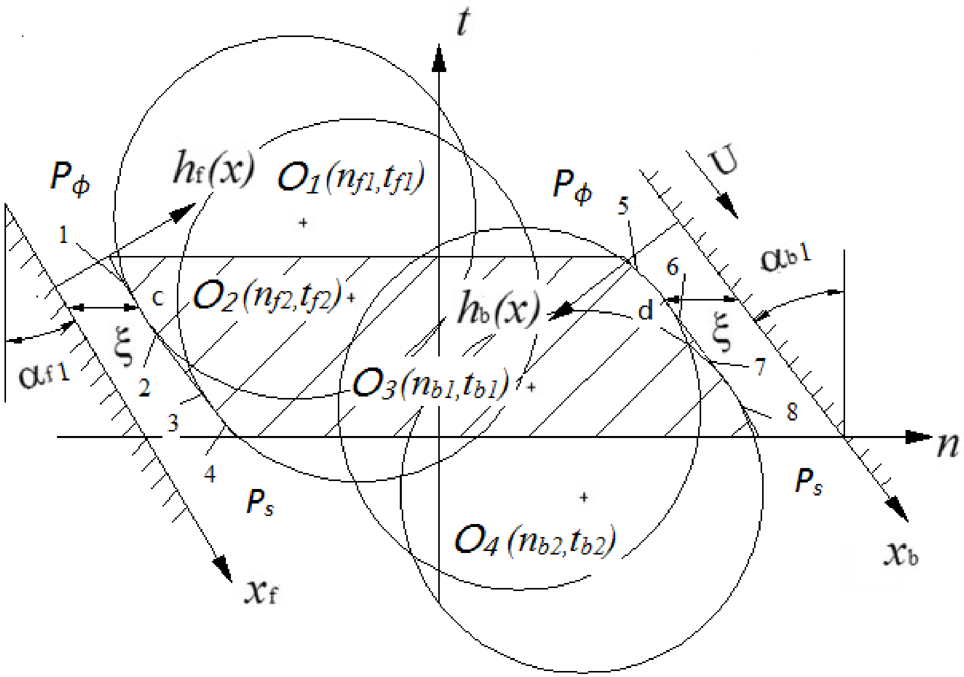

2. GEOMETRY MODEL

- The clearance functions for the front side of the tooth

$$h_f(t)=\begin{cases} h_f(t_1)+\dfrac{(t-t_1)\sin(\alpha_{f1}-\alpha_1)}{\cos(\alpha_1)} & t_1<t\le u \\ \xi\cos(\alpha_{f1})+r-r\cos(\alpha_{f1}-\arcsin(\dfrac{t_{f1}-t}{r})) & t_2\le t\le t_1 \\ h_f(t_2)+\dfrac{(t_2-t)\sin(\alpha_2-\alpha_{f1})}{\cos(\alpha_2)} & t_3\le t< t_2 \\ h_f(t_3)+\dfrac{(t_3-t)\sin(\dfrac{\arcsin(\frac{t_{f2}-t}{r})+\alpha_2}{2}-\alpha_{f1})}{\cos(\dfrac{\arcsin(\frac{t_{f2}-t}{r})+\alpha_2}{2})} & t_4\le t< t_3 \\ h_f(t_4)+\dfrac{(t_4-t)\sin(\alpha_4-\alpha_{f1})}{\cos(\alpha_4)} & 0\le t< t_4 \end{cases}$$

$$x(t)=\begin{cases} \dfrac{(u-t)\cos(\alpha_{f1}-\alpha_1)}{\cos(\alpha_1)} & t_1\le t\le u \\ x(t_1)+\dfrac{(t_1-t)\cos(\alpha_{f1}-\dfrac{\arcsin(\frac{t_{f1}-t}{r})+\alpha_1}{2})}{\cos(\dfrac{\arcsin(\frac{t_{f1}-t}{r})+\alpha_1}{2})} & t_c\le t< t_1 \\ x(t_c)+\dfrac{(t_c-t)\cos(\dfrac{\arcsin(\frac{t_{f1}-t}{r})-\alpha_{f1}}{2})}{\cos(\dfrac{\arcsin(\frac{t_{f1}-t}{r})+\alpha_{f1}}{2})} & t_2\le t< t_c \\ x(t_2)+\dfrac{(t_2-t)\cos(\alpha_2-\alpha_{f1})}{\cos(\alpha_2)} & t_3\le t< t_2 \\ x(t_3)+\dfrac{(t_3-t)\cos(\dfrac{\arcsin(\frac{t_{f2}-t}{r})+\alpha_2}{2}-\alpha_{f1})}{\cos(\dfrac{\arcsin(\frac{t_{f2}-t}{r})+\alpha_2}{2})} & t_4\le t< t_3 \\ x(t_4)+\dfrac{(t_4-t)\cos(\alpha_4-\alpha_{f1})}{\cos(\alpha_4)} & 0\le t< t_4 \end{cases}$$

2. GEOMETRY MODEL

- α_1 and α_4 are angles of the tangent lines when points 1 and 4 act as the meshing points

$$\begin{cases} \tan\alpha_1 = \dfrac{\omega_2 r_{2j}}{\omega_1 R_1} \\ \tan\alpha_4 = \dfrac{\omega_2 r_{2j}}{\omega_1 (a - r_{2j})} \end{cases}$$

- $\alpha_2=\alpha_3$.t_1~t_4 are the related height of the points

$$\begin{cases} t_i = t_{f1} - r\sin(\alpha_i) \quad i = 1,2 \\ t_i = t_{f2} - r\sin(\alpha_i) \quad i = 3,4 \end{cases}$$

2. GEOMETRY MODEL

● 2.3 Single-column Meshing Pair

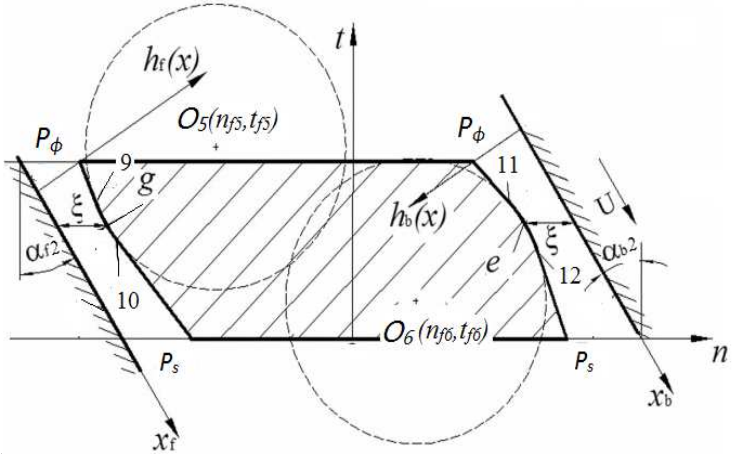

- The groove inclined angles (α_{f2}, α_{b2})

$$\begin{cases} \tan\alpha_{f2} = \dfrac{\omega_2 r_{2j}}{\omega_1 r_{2fj}} \\ \tan\alpha_{b2} = \dfrac{\omega_2 r_{2j}}{\omega_1 r_{2bj}} \end{cases}$$

- The clearance functions for the front side are

$$h_f(t) = \begin{cases} h_f(t_9) + \dfrac{(t-t_9)\sin(\alpha_{f2}-\alpha_9)}{\cos(\alpha_9)} & t_9 < t \le u \\ \xi\cos(\alpha_{f2}) + r - r\cos(\alpha_{f2} - \arcsin(\dfrac{t_{f5}-t}{r})) & t_{10} \le t \le t_9 \\ h_f(t_{10}) + \dfrac{(t_{10}-t)\sin(\alpha_{10}-\alpha_{f2})}{\cos(\alpha_{10})} & 0 \le t < t_{10} \end{cases}$$

$$x_f(t) = \begin{cases} \dfrac{(u-t)\cos(\alpha_{f2}-\alpha_9)}{\cos(\alpha_9)} & t_9 \le t \le u \\ x_f(t_9) + \dfrac{(t_{10}-t)\cos\left(\alpha_{f2} - \dfrac{\arcsin(\frac{t_{f5}-t}{r}) + \alpha_9}{2}\right)}{\cos\left(\dfrac{\arcsin(\frac{t_{f5}-t}{r}) + \alpha_9}{2}\right)} & t_g \le t < t_9 \\ x_f(t_g) + \dfrac{(t_g-t)\cos\left(\alpha_{f2} - \dfrac{\arcsin(\frac{t_{f5}-t}{r}) - \alpha_{f2}}{2}\right)}{\cos\left(\dfrac{\arcsin(\frac{t_{f5}-t}{r}) + \alpha_{f2}}{2}\right)} & t_{10} \le t < t_g \\ x_f(t_{10}) + \dfrac{(t_{10}-t)\cos(\alpha_{10}-\alpha_{f2})}{\cos(\alpha_{10})} & 0 \le t < t_{10} \end{cases}$$

2. GEOMETRY MODEL

- α_9, α_{10} are the angles of the tangent lines when points 9 and 10 act as the meshing points

$$\begin{cases} \tan\alpha_9 = \dfrac{\omega_2 r_{2j}}{\omega_1 R_1} \\ \tan\alpha_{10} = \dfrac{\omega_2 r_{2j}}{\omega_1 (a - r_{2j})} \end{cases}$$

- t_9 and t_{10} are the related height of the meshing points

$$t_i = t_{f5} - r\sin(\alpha_i) \quad i = 9,10$$

2. GEOMETRY MODEL

● 2.3 Lubrication Model

- The lubrication model introduced by Launder and Leschziner (1978) can be simplified

$$\frac{\mathrm{d}P(x)}{\mathrm{d}x}=\frac{6\mu U}{h(x)^2}-\frac{12\mu M}{\rho h(x)^3}+\frac{1.2M^2}{\rho h(x)^3}\cdot\frac{\mathrm{d}h(x)}{\mathrm{d}x}-\frac{0.133\rho U^2}{h(x)}\cdot\frac{\mathrm{d}h(x)}{\mathrm{d}x}$$

- Boundary condition

$$\begin{cases} x=x_0, P(x)=P_\phi \\ x=x_n, P(x)=P_s \end{cases}$$

P_ϕ is the gas pressure in the compressing chamber, P_s is the suction pressure

- The pressure distribution along the tooth surface in the convergent region

$$P(x)=P_\phi+\int_{x0}^{x}\frac{6\mu U}{h(x)^2}\mathrm{d}x-\frac{12\mu M}{\rho}\int_{x0}^{x}\frac{1}{h(x)^3}\mathrm{d}x$$
$$-\frac{1.2M^2}{2\rho}\left(\frac{1}{h(x)^2}-\frac{1}{h(x_0)^3}\right)-0.133\rho U^2[\ln h(x)-\ln h(x_0)]$$

$$M=\frac{\frac{12\mu}{\rho}\int_{x0}^{x_n}\frac{1}{h(x)^3}\mathrm{d}t-\sqrt{\left(\frac{12\mu}{\rho}\int_{x0}^{x_n}\frac{1}{h(x)^3}\mathrm{d}t\right)^2+\frac{2\cdot 1.2}{\rho}\left(\frac{1}{h(x_n)^2}-\frac{1}{h(x_0)^2}\right)N}}{\frac{1.2}{\rho}\left(\frac{1}{h(x_0)^2}-\frac{1}{h(x_n)^2}\right)}$$

2. GEOMETRY MODEL

- The relative velocity between the meshing pair *U*

$$U = \sqrt{(\omega_2 r_{2j})^2 + (\omega_1 r_{1(f,b)j})^2}$$

- Component forces caused by the oil film and the gas force, applied on the engaged element dl and the gas force, applied on the unengaged element *dl*

$$\begin{cases} F_{oij}' = \cos\alpha \cdot \int_{x_0}^{x_n} P(x)dx \\ F_{gi} = \cos\alpha \cdot \int_{x_n}^{x_s} P_s dx \end{cases} \qquad F_{gi}' = u \cdot P_s$$

- The torques applied on each side of the tooth

$$\begin{cases} T_{fi} = \int_{l_f}^{L} F_{foij}' \cdot r_{2j}(l)dl + \int_{l_f}^{L} F_{fgi} \cdot r_{2j}(l)dl + \int_{0}^{l_f} F_{fgi}' \cdot r_{2j}(l)dl \\ T_{bi} = \int_{l_b}^{L} F_{oijb}' \cdot r_{2j}(l)dl + \int_{l_b}^{L} F_{bgi} \cdot r_{2j}(l)dl + \int_{0}^{l_b} F_{bgi}' \cdot r_{2j}(l)dl \end{cases}$$

- The total torque applied on the star-wheel

$$T = \sum_{1}^{4} T_i \qquad T_i = T_{bi} - T_{fi}$$

3. RESULTS

- Dimensions of the single screw compressor

Table 1: Dimensions of the single screw compressor

Main Parameter	Value	Main Parameter	Value
Screw rotor radius R_1/mm	65	Tooth length L/mm	30
Star-wheel radius R_2/mm	61	Center distance a/mm	96
Tooth width b/mm	18	Envelope column radius r/mm	6
Rotating speed $/ r \cdot min^{-1}$	2970	Discharge pressure $P_{out}/10^5 Pa$	10
Design clearance ξ/mm	0.04		

3. RESULTS

- Design parameters related to the two different profiles

β_f =2.327°, β_b=-2.298°

Table 2: Design parameters

Parameter	***n/mm***	***t /mm***
Tooth top of Column O_1	-4.754	7.292
Column O_2	-2.674	4.542
Column O_3	2.674	0.958
Tooth top of Column O_4	4.739	-1.792
Column O_5	-2.674	4.542
Column O_6	2.674	0.958

3. RESULTS

- Pressure distributions of the two types meshing pair under the discharge starting rotation angle (ϕ_2=35°) at the tooth top

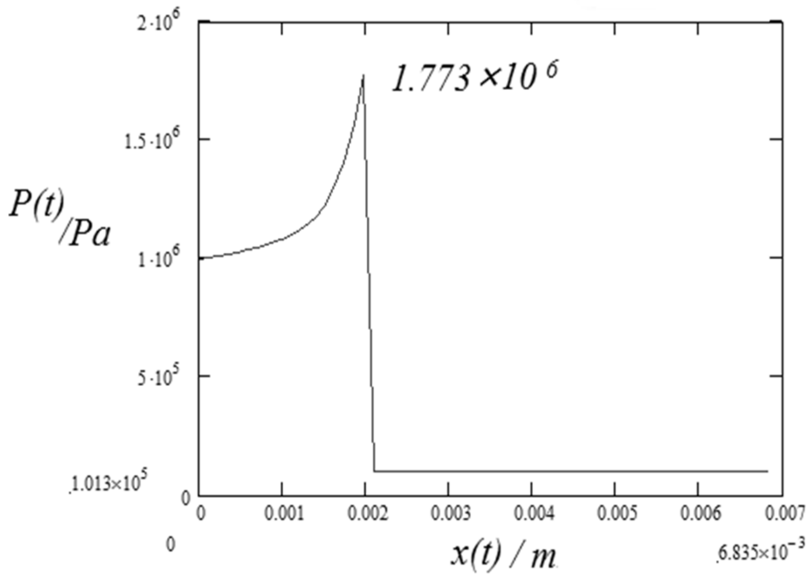

(a) Pressure distribution for double-column meshing pair

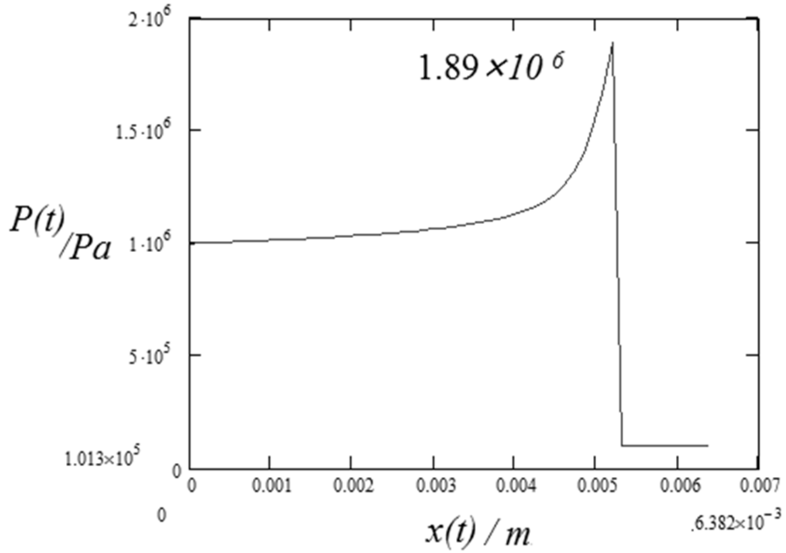

(b) Pressure distribution for single-column meshing pair

3. RESULTS

- The total torques of the two types meshing pair

For the double-column, the total torque changes from 1.3 N·m to 3.7 N·m. For the single-column, the total torque changes from 2.92 N·m to 4.5 N·m.

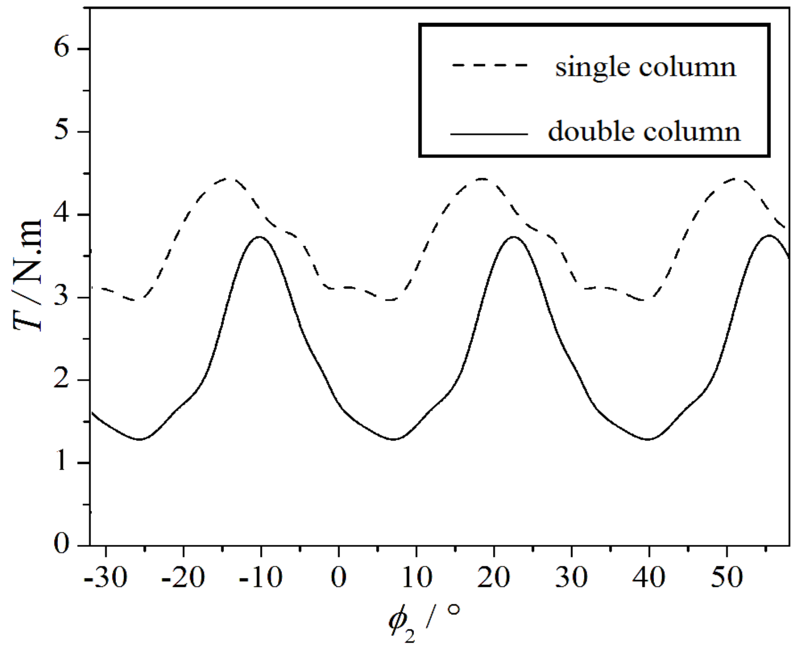

4. CONCLUSIONS

- The pressure increases to a peak value from the start of the convergent region to the meshing point.
- The total torques caused by the oil film forces are unbalanced, which would lead to a deflection of the tooth in order to regain balance. Furthering result in changes in the clearances between the meshing pair and may cause metal contact of the meshing pair reducing the operation life.
- The total torque generated by the double-column meshing pair profile is smaller than that of the single-column at any same rotation angle, which indicates the double-column meshing pair profile has a better hydrodynamic lubrication state and a longer operation life.
- The analysis can also be used to optimize the meshing pair profile design for single screw compressors.

Thank you!